HETEROCYCLES, Vol. 76, No. 2, 2008, pp. 1369 - 1380. © The Japan Institute of Heterocyclic Chemistry
Received, 9th April, 2008, Accepted, 30th June, 2008, Published online, 7th July, 2008. COM-08-S(N)102

THE MCD SPECTROSCOPY OF CORROLAZINES AND TRIAZATETRABENZOCORROLES

John Mack,[a] Masaru Bunya,[a] David Lansky,[b] David P. Goldberg,*[b] and Nagao Kobayashi*[a]

[a]Department of Chemistry, Faculty of Graduate Science, Tohoku University, Sendai 980-8578, Japan
[b]Department of Chemistry, Johns Hopkins University, 3400 N. Charles Street, Baltimore, Maryland, 21218, United States
*E-mail addresses: nagaok@mail.tains.tohoku.ac.jp, dpg@jhu.edu

Abstract – We report the first MCD spectral data for free base corrolazine and a transition metal corrolazine complex. A detailed analysis of the MCD and UV-visible absorption spectroscopy of these compounds and phosphorous corrolazine and triazatetrabenzocorroles is carried out based on the results of TD-DFT calculations and an application of Michl's perimeter model.

INTRODUCTION

Over the last decade there has been increasing interest in the synthesis and spectroscopy of metal corrole complexes.[1,2] The major structural difference between the corrole (Crl) and porphyrin (P) ligands is the introduction of a direct C−C bond between two neighboring pyrrole rings. The corrole ligand forms a trianion when fully deprotonated, as opposed to a dianion for porphyrins, and this extra negative charge contributes to the corroles' ability to stabilize higher oxidation states of central metal ions.[3] Less attention has been paid until recently[4] to aza-nitrogen analogues of the porphyrazines (Pz) and phthalocyanines (Pc), the corrolazines (Cz) and triazatetrabenzocorroles (TBC) (Figure 1). Fujiki *et al.*[5] reported the first formation of a stable TBC complex in 1986. $(OH^{-})Ge^{IV}TBC$ was formed *via* a ring-contraction reaction from $(Cl^{-})_2Ge^{IV}Pc$ in the presence of reducing agents such as $NaBH_4$ and H_2Se. Li *et al.*[6] subsequently used similar approaches to form $(X^{-})Si^{IV}TBC$ and $(O^{2-})P^{V}TBC$ complexes, while Kobayashi *et al.*[7] have reported the formation of $(X^{-})Si^{IV}TBC$ and $(X^{-})Si^{IV}Cz$.[8] The syntheses and properties of a wide range of Cz and TBC complexes have also been studied in depth by Goldberg and coworkers.[1] In this paper we explore the extent to which the MCD spectroscopy of corrolazines and triazatetrabenzocorroles can be

rationalized based on Gouterman's 4-orbital model[9] and Michl's perimeter model.[10] The prospects for carrying out detailed analyses of the optical spectra of transition metal complexes are assessed through an analysis of the MCD spectra of free base octakis(*p-tert*-butylphenyl)corrolazine (**H_3tBuPh$_8$Cz**), P^V octakis(*p-tert*-butylphenyl)corrolazine (**[(OH$^-$)P^{V}tBuPh$_8$Cz]$^+$OH$^-$**), Mn^{III} octakis(*p-tert*-butylphenyl)corrolazine (**Mn^{III}tBuPh$_8$Cz**) and 3,6,10,13,17,20,24,27-octabutoxytriaza-tetrabenzocorrole (**(OCH$_3^-$)$_2$P^{V}nBuO$_8$TBC**) based on TD-DFT calculations of related model compounds.

RESULTS AND DISCUSSION

The absorption and MCD spectra of **H_3tBuPh$_8$Cz**, **[(OH$^-$)P^{V}tBuPh$_8$Cz]$^+$OH$^-$**, **Mn^{III}tBuPh$_8$Cz**, **(OCH$_3^-$)$_2$P^{V}nBuO$_8$TBC** and ZnPc are shown in Figure 1. Two intense absorption bands are observed in the visible region at 679 and 460 nm in the case of **H_3tBuPh$_8$Cz**, at 638 and 445 nm for **[(OH$^-$)P^{V}tBuPh$_8$Cz]$^+$OH$^-$**, at 685 and 435 nm for **Mn^{III}tBuPh$_8$Cz** and at 735 and 520 nm for **(OCH$_3^-$)$_2$P^{V}nBuO$_8$TBC**. The intensity scales for the MCD spectra of the Cz and TBC spectra are between one and three orders of magnitude less intense than is the case with ZnPc (Figure 1). The derivative-shaped $\mathcal{A}_1$ terms observed for ZnPc are replaced in the MCD spectra of **H_3tBuPh$_8$Cz**,

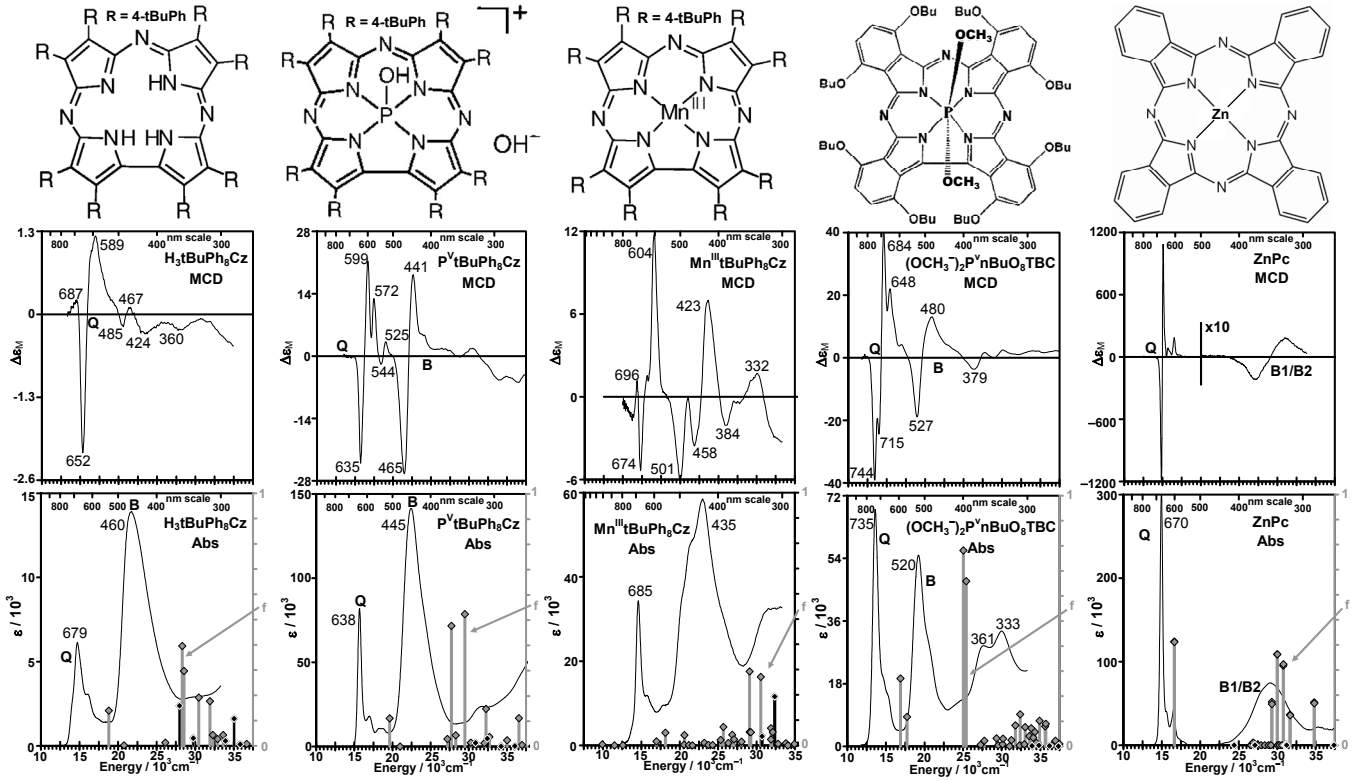

Figure 1. The molecular structures (TOP) and MCD and UV-visible absorption spectra in dimethylformamide at 298 K (BOTTOM) of **H_3tBuPh$_8$Cz**, **[(OH$^-$)P^{V}tBuPh$_8$Cz]$^+$OH$^-$**, **Mn^{III}tBuPh$_8$Cz**, **(OCH$_3^-$)$_2$P^{V}nBuO$_8$TBC** and ZnPc. An energy scale is used (a wavelength scale is also provided at the top of each plot) and the wavelengths of the major bands are annotated. Calculated TD-DFT absorption spectra for H_3Cz, [(OH$^-$)P^{V}Cz]$^+$, (OH$^-$)$_2$P^{V}TBC model compounds and ZnPc are plotted against the right hand axes. Bands arising from transitions to nπ* states are denoted by black diamonds.

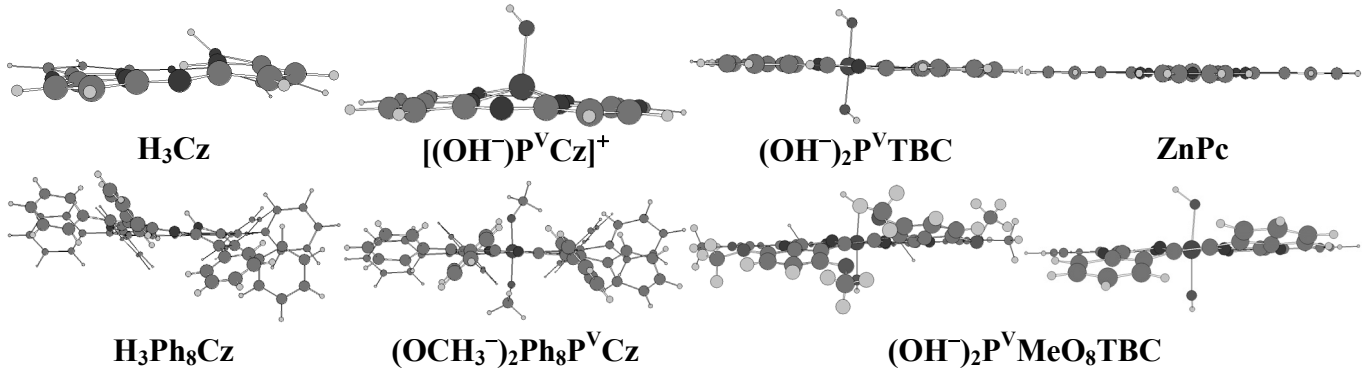

Figure 2. The B3LYP optimized structures of H_3Cz, $[(OH^-)P^VCz]^+OH^-$, $(OH^-)_2P^VTBC$ and ZnPc (TOP) and H_3Ph_8Cz, $(OCH_3^-)_2Ph_8P^VCz$ and $(OH^-)_2P^VMeO_8TBC$ model compounds (BOTTOM). Structures with and without OMe groups are shown in the case of $(OH^-)_2P^VMeO_8TBC$. The view is towards the direct C–C bond between neighboring pyrroles.

$[(OH^-)P^VtBuPh_8Cz]^+OH^-$ and **$(OCH_3^-)_2P^VnBuO_8TBC$** by coupled oppositely-signed Gaussian-shaped $\mathcal{B}_0$ terms. The ground–states of divalent, D_{4h} symmetry MP and MPc complexes are typically non–degenerate ($^1A_{1g}$), while the accessible $\pi \rightarrow \pi^*$ excited states are orbitally degenerate (^1E_u).[9] The MCD spectra are therefore usually dominated by intense *x/y*–polarized derivative-shaped Faraday $\mathcal{A}_1$ terms. In the case of Cz and TBC complexes the main four-fold axis of symmetry is removed (Figure 1). Complexes with symmetry lower than C_3, D_{2d} and S_4 symmetry give rise to zero–field split oppositely–signed coupled Faraday $\mathcal{B}_0$ terms, which are typically weaker than Faraday $\mathcal{A}_1$ terms since there is a $1/\Delta E_{KJ}$ dependence, where ΔE_{KJ} is the energy difference between the excited states mixed by the applied magnetic field based on a magnetic dipole transition moment.[11] The intensity of the MCD bands is weakest in the case of **H_3tBuPh_8Cz** where steric hindrance between the three protonated pyrrole nitrogens results in marked non-planarity disrupting the orbital angular momentum (OAM) properties of the heteroaromatic properties of the π–system (Figure 2).

In the 1950s, Moffitt[12] demonstrated that the OAM properties of porphyrinoids are best understood in terms of a high symmetry parent hydrocarbon since the nodal patterns of the main π–system MOs are retained when the symmetry is lowered by perturbations to the structure such as the incorporation of heteroatoms and fused rings (Figure 3). In the case of the $C_{15}H_{15}^{3-}$ parent perimeter of Cz and TBC complexes, the MOs are arranged in an $M_L = 0, \pm1, \pm2, \pm3, \pm4, \pm5, \pm6, \pm7$ sequence in ascending energy similar to the $M_L = 0, \pm1, 2$ sequence observed for the π–MOs of benzene. In a directly analogous manner to the $C_{16}H_{16}^{2-}$ parent perimeter of metal porphyrinoid complexes, the HOMO has an M_L value of ±4, therefore, while the LUMO has an M_L value of ±5. This is reflected in the number of nodal planes (Figure 3). In the context of the porphyrins and phthalocyanines, Gouterman's 4-orbital model[9] predicts a forbidden bands arising from the $\Delta M_L = \pm9$ transitions and allowed bands arising from the $\Delta M_L = \pm1$ transitions, referred to as the Q and B (or Soret) bands, respectively. Since there is a marked relative

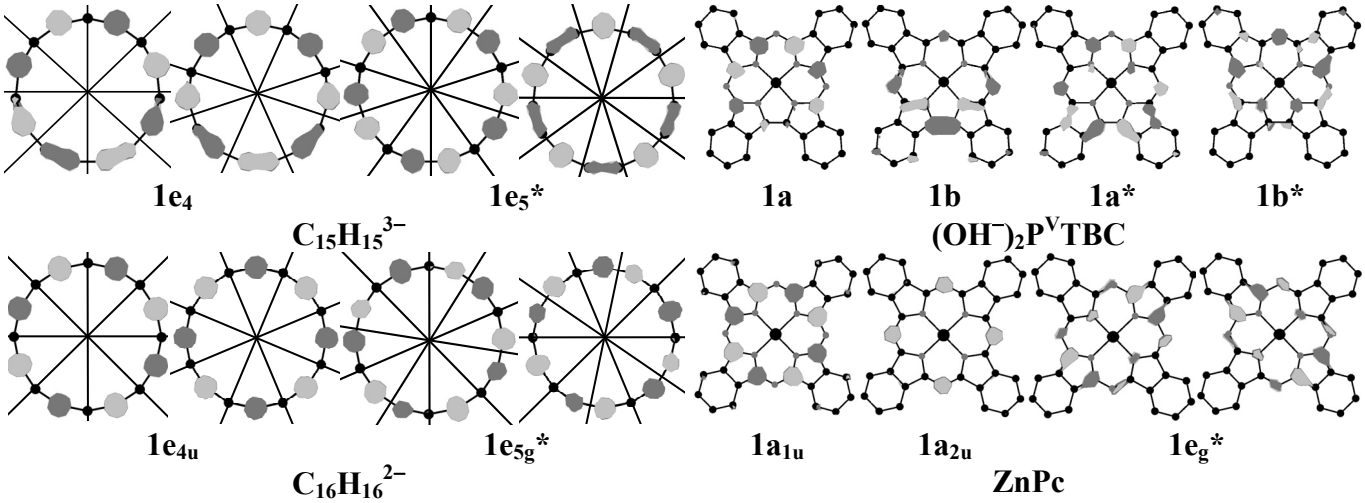

Figure 3. The nodal patterns of the four frontier π−MOs of $C_{15}H_{15}^{3-}$, $C_{16}H_{16}^{2-}$, $(OH^-)_2P^VTBC$ and ZnPc at an isosurface value of 0.05 a.u.. The nodal patterns shown for $C_{15}H_{15}^{3-}$ and $C_{16}H_{16}^{2-}$ are retained on the inner ligand perimeters of $(OH^-)_2P^VTBC$ and ZnPc as predicted by Michl's perimeter model.[10]

intensification of the lowest energy π → π* bands of Cz and TBC complexes in the MCD spectrum due to the larger induced magnetic moments, Gouterman's band nomenclature is clearly still applicable (Figure 1). Michl[10] has demonstrated that the sign sequences of coupled pairs of oppositely−signed Faraday $\mathcal{B}_0$ terms in the MCD spectra of aromatic and heteroaromatic cyclic polyenes (which replace the $\mathcal{A}_1$ terms when the *x/y*−degeneracy of the major π → π* transitions is broken) can be predicted in qualitative terms based on the relative magnitudes of the energy separations of the four frontier π-MOs arising from the HOMOs and LUMOs (ΔHOMO and ΔLUMO) of the parent perimeter. When ΔLUMO < ΔHOMO, as is the case with most tetraazaporphyrinoids, a –ve / +ve sequence is anticipated in $\mathcal{B}_0$ term intensity in ascending energy, while a +ve / –ve sequence is anticipated when ΔLUMO > ΔHOMO. The sign sequence is determined by whether the effective charge, which circulates on the perimeter in either a left or a right handed manner upon the absorption of an incident chiral photon, is positive or negative. The calculated energies of the frontier π−system MOs and the predicted ΔHOMO and ΔLUMO values for $C_{16}H_{16}^{2-}$, zinc porphyrin (ZnP), zinc porphyrazine (ZnPz), ZnPc, $C_{15}H_{15}^{3-}$ and for free base corrole (H_3C) and corrolazine (H_3Cz), $(OH^-)_2P^VCz$, $[(OH^-)P^VCz]^+$, $(OH^-)_2P^VTBC$ and $(OH^-)_2P^VMeO_8TBC$ model compounds and ion are shown schematically in Tables 1 and 2. The MOs in Table 1 are ordered relative to the corresponding ZnPc orbital based on the nodal patterns, which Michl[10] has demonstrated are retained by cyclic perimeters even after perturbations to the structure, so that the one electron transitions responsible for the bands within the calculated UV-visible spectra, Table 3, can be readily compared despite the different molecular symmetries.

It is not currently possible to calculate quantitative values for the three Faraday terms based on the TD-DFT calculations provided in commercially available software packages so the sign sequences observed for the MCD band can only be predicted qualitatively based on the predicted MO energies.

Table 1. The calculated energies and symmetries of frontier MOs of $C_{16}H_{16}^{2-}$ (CP_{16}), ZnP, ZnPz, ZnPc, $C_{15}H_{15}^{3-}$ (CP_{15}), H_3Crl, H_3Cz, $(OH^-)_2P^VCz$, $[(OH^-)P^VCz]^+$, $(OH^-)_2P^V$TBC and $(OH^-)_2P^V$MeO$_8$TBC. MOs arising from the lone pairs of the aza-nitrogens are marked with an N superscript. The four frontier π–MOs associated with Gouterman's 4-orbital model are in bold.

M_L	CP_{16}		ZnP	ZnPz	ZnPc		CP_{15}	H_3Crl		H_3Cz		$(OH^-)_2P^VCz$		$[(OH^-)P^VCz]^+$		$(OH^-)_2P^V$TBC		
	(D_{16h})		(D_{4h})		(D_{4h})		(D_{15h})	(C_1)		(C_1)		(C_{2v}(III))		(C_s)		(C_{2v}(III))		MeO$_8$
±6	8.68	$1b_{2u}$*	1.36	0.64	$1b_{2u}$*	–0.87	13.58	4a*	1.21	4a*	0.76	$2a_2$*	0.64	4a'	–2.76	$2a_2$*	–0.86	
	8.68	$1b_{1u}$*	–0.54	–1.46	$1b_{1u}$*	–1.13	13.58	3a*	0.19	3a*	–0.33	$2b_2$*	–0.20	2a"	–4.68	$2b_2$*	–0.90	(C_1)
±5	**5.87**	**$1e_g$***	**–2.14**	**–3.13**	**$1e_g$***	**–2.79**	**10.64**	**2a***	**–1.54**	**2a***	**–2.24**	**$1b_2$***	**–2.36**	**1a"***	**–6.28**	**$1b_2$***	**–2.25**	**2a*** **–2.28**
	5.87	**$1e_g$***	**–2.14**	**–3.13**	**$1e_g$***	**–2.79**	**10.64**	**1a***	**–2.09**	**1a***	**–2.85**	**$1a_2$***	**–2.88**	**1a'***	**–6.61**	**$1a_2$***	**–2.45**	**1a*** **–2.52**
±4	**2.80**	**$1a_{1u}$**	**–5.21**	**–5.79**	**$1a_{1u}$**	**–4.94**	**7.35**	**2a**	**–5.02**	**1a**	**–5.38**	**$1a_2$**	**–5.54**	**1a'**	**–9.34**	**$1a_2$**	**–4.75**	**1a** **–4.76**
	2.80	**$1a_{2u}$**	**–5.22**	**–6.94**	**$1a_{2u}$**	**–6.76**	**7.35**	**1a**	**–4.80**	**2a**	**–5.96**	**$1b_2$**	**–6.00**	**1a"**	**–9.95**	**$1b_2$**	**–5.61**	**2a** **–5.56**
	---	$1b_{1g}^N$	–6.35	–6.61	$1b_{1g}^N$	–6.66	---	$5a^N$	–7.11	$5a^N$	–7.27	$2b_1^N$	–9.66	$7a'^N$	–13.75	$2b_1^N$	–9.18	
	---	$1b_{2u}$	–6.59	–7.10	$1b_{2u}$	–6.69	---	3a	–6.23	3a	–6.68	$3a_2$	–7.29	2a'	–11.04	$3a_2$	–6.88	
	---	$1e_g$	–6.60	–7.14	$1e_g$	–6.72	---	6a	–7.19	8a	–7.69	$2b_2$	–6.95	2a"	–11.28	$2b_2$	–6.69	
	---	$1e_g$	–6.60	–7.14	$1e_g$	–6.72	---	4a	–6.89	6a	–7.51	$2a_2$	–7.07	3a'	–11.37	$2a_2$	–6.78	
	---	---	---	---	$2e_g$	–6.94	---	---	---	---	---	---	---	---	---	$4b_2$	–6.95	
	---	---	---	---	$2e_g$	–6.94	---	---	---	---	---	---	---	---	---	$4a_2$	–7.03	
	---	$1b_{2g}^N$	---	–7.13	$1b_{2g}^N$	–6.98	---	---	---	$4a^N$	–7.16	$1a_1^N$	–7.53	$4a'^N$	–11.41	$1a_1^N$	–7.43	
	---	---	---	---	$1b_{1u}$	–6.98	---	---	---	---	---	---	---	---	---	$3b_2$	–6.91	
	---	$2a_{2u}$	–7.00	–7.55	$2a_{2u}$	–7.02	---	7a	–7.24	7a	–7.60	$3b_2$	–7.48	4a"	–11.76	$5b_2$	–7.16	
	---	$1e_u^N$	---	–7.61	$1e_u^N$	–7.48	---	---	---	$9a^N$	–7.89	$1b_1^N$	–7.80	$3a"^N$	–11.58	$1b_1^N$	–7.72	
	---	$1e_u^N$	---	–7.61	$1e_u^N$	–7.48	---	---	---	---	---	---	---	---	---	---	---	
	---	---	---	---	$2a_{1u}$	–7.52	---	---	---	---	---	---	---	---	---	$5a_2$	–7.52	
	---	$1a_{1g}^N$	---	–8.39	$1a_{1g}^N$	–8.25	---	---	---	$10a^N$	–8.07	$2a_1^N$	–8.29	$5a'^N$	–12.13	$1a_1^N$	–8.20	
±3	0.61	$2e_g$	–7.52	–8.79	$3e_g$	–8.59	4.99	8a	–7.30	12a	–8.58	$5a_2$	–8.70	5a"	–12.42	$7a_2$	–8.64	
	0.61	$2e_g$	–7.52	–8.79	$3e_g$	–8.59	4.99	9a	–7.40	11a	–8.47	$5b_2$	–9.30	6a'	–12.62	$7b_2$	–8.68	

Table 2. The predicted ΔHOMO (ΔH), ΔLUMO (ΔL), ΔH–ΔL and HOMO – LUMO band gap (H – L) values in eV of $C_{16}H_{16}^{2-}$ (CP_{16}), ZnP, ZnPz, ZnPc, $C_{15}H_{15}^{3-}$ (CP_{15}), H_3Crl, H_3Cz, $(OH^-)_2P^VCz$, $[(OH^-)P^VCz]^+$ and $(OH^-)_2P^V$TBC. Values for H_3Ph_8Cz, $(OCH_3^-)_2P^VPh_8Cz$ and $(OH^-)_2P^V$MeO$_8$TBC, Figures 2 and 4, are also provided to illustrate the effects of peripheral substitution.

	CP_{16}	ZnP	ZnPz	ZnPc	CP_{15}	H_3Crl	H_3Cz	$(OH^-)_2P^VCz$	$[(OH^-)P^VCz]^+$	H_3Ph_8Cz	$(OCH_3^-)_2P^VPh_8Cz$	$(OH^-)_2P^V$TBC	$(OH^-)_2P^V$MeO$_8$TBC
ΔL	0.00	0.00	0.00	0.00	0.00	0.55	0.61	0.52	0.33	0.63	0.52	0.20	0.24
ΔH	0.00	0.01	1.15	1.82	0.00	0.22	0.58	0.46	0.61	0.38	0.34	0.86	0.80
ΔH–ΔL	0.00	0.01	1.15	1.82	0.00	–0.33	–0.02	–0.06	0.28	–0.25	–0.18	0.66	0.56
H – L	3.07	3.07	2.66	2.15	3.29	2.71	2.53	2.66	2.73	2.32	2.32	2.30	2.24

The four one-electron transitions associated with Gouterman's 4-orbital model are highlighted in bold. The TD-DFT calculations predict that these transitions continue to play a major role in the case of the H_3Cz, $(OH^-)_2P^VCz$ and $(OH^-)_2P^VTBC$ model compounds. The major bands in the UV-visible region are assigned to the Q and B transitions on this basis (Figure 1). The calculated spectra are plotted against the secondary right hand axis to provide a comparison with the observed optical spectra for **H_3tBuPh$_8$Cz**, **[(OH$^-$)P^{V}tBuPh$_8$Cz]$^+$OH$^-$** and **(OCH$_3^-$)$_2$P^{V}nBuO$_8$TBC** (Figure 1). Since the aza-nitrogens have large MO coefficients, the removal of an electronegative aza-nitrogen results in a marked destabilization of the $1a_{2u}$ 2nd HOMO of ZnPc (Table 1). In contrast, the energy of the $1a_{1u}$ HOMO of ZnPc is largely unaffected since these atoms lie on nodal planes. As a result the ΔHOMO value of the Cz and TBC compounds is substantially reduced, while the ΔLUMO value is relatively low since the effect of the perturbation to the structure is identical along both the *x*- and *y*-axes. In the case of **[(OH$^-$)P^{V}tBuPh$_8$Cz]$^+$OH$^-$** the –ve / +ve sign sequence observed for the pseudo-$\mathcal{A}_1$ terms that comprise the Q and B bands in the MCD spectrum (Figure 1), can be readily accounted for based on the predictions that ΔHOMO > ΔLUMO and ΔLUMO ≈ 0 (Tables 1 – 3). The positive and negative $\mathcal{B}_0$ terms in the Q band region at 572, 544 and 525 nm are almost certainly vibrational in origin. In the calculation for H_3Cz and $(OH^-)_2P^VCz$, the reduction in the ΔHOMO value is predicted to result in soft MCD chromophores where ΔHOMO ≈ ΔLUMO. Under these circumstances the π-system essentially mimics the properties of a high symmetry species.[10] The spectra of **H_3tBuPh$_8$Cz** and **[(OH$^-$)P^{V}tBuPh$_8$Cz]$^+$OH$^-$** are clearly not consistent with a soft MCD chromophore, as the Q bands, which would normally be expected to be fully forbidden, have significant absorption intensity. When the 5-coordinate $[(OH^-)P^VCz]^+$ species predicted by NMR spectroscopy[4] is taken into consideration, instead, however, the ΔHOMO value is predicted to be significantly greater than the ΔLUMO value. An explanation for **H_3tBuPh$_8$Cz** is less straightforward. TD-DFT calculations for ZnP and zinc tetraphenylporphyrin have recently been found to be inconsistent with the observed spectral properties so it may be related to problems associated with the calculation technique.[13] The complex sequence of signs observed in the Q and B band regions of **H_3tBuPh$_8$Cz** is probably related to the presence of multiple conformers and the quenching of the OAM properties of the π–system by the non-planarity induced by the steric hindrance between the three protonated pyrrole nitrogens (Figure 2).

The removal of an aza-nitrogen from the Pc ligand to form the TBC ligand has a substantial impact on the electronic structure and optical spectroscopy. The energy gap between the Q and B bands of **(OCH$_3^-$)$_2$P^{V}nBuO$_8$TBC** is substantially narrower than is the case with ZnPc and there is a marked red shift and sharpening of the B bands (Figure 1). There is also a lifting of the degeneracy of the LUMOs in Michl's perimeter model and a marked reduction in the ΔHOMO value (Tables 1 and 2). It should be

Table 3. TD-DFT calculated spectra of H_3Cz, $[(OH^-)P^VCz]^+$, $(OH^-)_2P^VTBC$, $(OH^-)_2P^VMeO_8TBC$ and ZnPc. The symmetry of the states (Sym.), energies of the absorption bands in wavenumbers (cm^{-1}) and nanometers (nm), oscillator strengths (f), percentage contribution of one-electron transitions and band assignments are provided from left to right in ascending energy for bands (#) with an oscillator strength greater than 0.1 in the case of the UV region of the ZnPc spectrum. One-electron transitions associated with Gouterman's 4-orbital model[9] and Michl's perimeter model[10] are shown in bold. Lone pair orbitals are marked with an N superscript.

H_3Cz						
#	**Sym.**	**10^3 cm^{-1}**	**nm**	**f**	**One-electron Transitions (%)**	**Band**
1	^1A					
2	^1A	18.8	532	0.14	**66% 1a*←1a + 25% 2a*←2a** +...	Q
3	^1A	20.8	481	0.00	**49% 2a*←1a + 46% 1a*←2a** +...	Q
4	^1A	26.1	383	0.01	85% 1a*←3a +...	
5	^1A	28.0	357	0.16	71% 1a*←$4a^N$ +...	n→π*
6	^1A	28.3	353	0.40	17% 1a*←$4a^N$ **+ 14% 2a*←2a + 13% 2a*←1a + 13% 1a*←2a** +...	B
7	^1A	28.5	350	0.30	**26% 2a*←2a** + 21% 2a*←3a +...	B
$[(OH^-)P^VCz]^+$						
#	**Sym.**	**10^3 cm^{-1}**	**nm**	**f**	**One-electron Transitions (%)**	**Band**
1	$^1A'$					
2	$^1A'$	19.8	504	0.08	**67% 1a'*←1a' + 28% 1a"*←1a"** +...	Q
3	$^1A"$	20.7	482	0.01	**61% 1a"*←1a' + 37% 1a'*←1a"** +...	Q
4	$^1A"$	28.7	349	0.54	**39% 1a'*←1a" + 16% 1a"*←1a'** +...	B
5	$^1A'$	29.4	340	0.45	**51% 1a"*←1a"** + 12% 1a'*←2a' **+ 8% 1a' *←1a'** +...	B
$(OH^-)_2P^VTBC$						
#	**Sym.**	**10^3 cm^{-1}**	**nm**	**f**	**One-electron Transitions (%)**	**Band**
1	$^1A_1$					
2	$^1A_1$	16.9	592	0.27	**72% $1a_2$*←$1a_2$ + 18% $1b_2$*←$1b_2$** +...	Q
3	$^1B_1$	17.7	564	0.12	**70% $1b_2$*←$1a_2$ + 22% $1a_2$*←$1b_2$** +...	Q
4	$^1B_1$	25.0	400	0.78	**62% $1a_2$*←$1b_2$ + 9% $1b_2$*←$1a_2$** +...	B
5	$^1A_1$	25.4	394	0.66	**71% $1b_2$*←$1b_2$** + **5% $1a_2$*←$1a_2$** +...	B
$(OH^-)_2P^VMeO_8TBC$						
#	**Sym.**	**10^3 cm^{-1}**	**nm**	**f**	**One-electron Transitions (%)**	**Band**
1	^1A					
2	^1A	15.0	668	0.28	**75% 1a*←1a + 10% 2a*←2a** +...	Q
3	^1A	16.1	622	0.12	**69% 2a*←1a + 21% 1a*←2a** +...	Q
4	^1A	20.5	489	0.55	**62% 1a*←2a + 11% 2a*←1a** +...	B
5	^1A	21.6	463	0.36	**76% 2a*←2a** + 4% 1a*←4a + **3% 1a*←1a** +...	B

ZnPc						
#	Sym.	10^3 cm^{-1}	nm	f	One-electron Transitions (%)	Band[14]
1	$^1A_{1g}$					
2, 3	^1E_u	16.6	602	0.41	72% **$1e_g^*\leftarrow 1a_{1u}$** + 10% **$1e_g^*\leftarrow 1a_{2u}$** +...	Q
4, 5	$^1A_{2u}$	24.4	410	0.00	98% $1e_g^*\leftarrow 1b_{1g}{}^N$ +...	n→π*
8, 9	^1E_u	26.9	372	0.01	88% $1e_g^*\leftarrow 1b_{2u}$ +...	2nd π→π*
4, 5	$^1A_{2u}$	27.1	369	0.00	98% $1e_g^*\leftarrow 1b_{2g}{}^N$ +...	n→π*
17, 18	^1E_u	29.3	341	0.17	46% $1e_g^*\leftarrow 2a_{2u}$ + 40% **$1e_g^*\leftarrow 1a_{2u}$** +...	
19, 20	^1E_u	30.0	333	0.36	78% $1e_g^*\leftarrow 1b_{1u}$ + 10% **$1e_g^*\leftarrow 1a_{2u}$** +...	B1
25, 26	^1E_u	30.8	325	0.32	36% $1e_g^*\leftarrow 2a_{2u}$ + 28% **$1e_g^*\leftarrow 1a_{2u}$** + 12% $1e_g^*\leftarrow 2a_{1u}$ +...	B2
31, 32	^1E_u	31.7	316	0.12	88% $2e_g^*\leftarrow 1a_{1u}$ +...	N
33, 34	^1E_u	34.8	287	0.17	80% $1e_g^*\leftarrow 2a_{1u}$ +...	L

noted that, in both instances charge transfer between the metal and the ligand is not predicted to be a significant factor in the 300 – 1000 nm region. Zn(II) complexes are often used to model the electronic structures of porphyrinoid ligands, since Zn^{II} has a closed shell d^{10} configuration.[13] In the late 1960s, Hochstrasser[14] postulated, based on empirical observations, that significant band broadening is observed for the π → π* bands of heteroaromatic π–systems arising from ππ* excited states, which lie at higher energy than nπ* states. This has been used to account for the significant band broadening that is observed for the B1 and B2 bands of MPc complexes relative to the Q band since weak n → π* transitions are predicted to lie to the red of the B1/B2 band envelope (Figure 1).[15] In the case of **$(OCH_3^-)_2P^VnBuO_8TBC$**, the band widths of the main Faraday $\mathcal{B}_0$ terms in the Q and B band regions are clearly much more comparable than is the case in the ZnPc spectrum. The energies of the n → π* transitions of **$(OCH_3^-)_2P^VnBuO_8TBC$** are predicted to lie well to the blue of the B bands (Figure 1 and Table 3). The main reason for this is the effect of removing an aza-nitrogen on the energies of the non-bonding MOs associated with the aza-nitrogen lone pairs (Table 1). There is also a marked red shift in the energy of the B band. The fact that the ΔHOMO value is significantly reduced relative to the Pc ligand is probably the key factor. In the case of zinc porphyrinoids, a small ΔHOMO value has been found to result in a lower level of configuration interaction between the B and higher energy ππ* excited states.[13] The unusually high ΔHOMO value of Pc results in a mixing of the forbidden and allowed properties of the Q and B bands and extensive configuration interaction between the B and higher energy ππ* states. This results in multiple intense bands in the UV-region that are usually labeled B1 and B2, Table 3, which lie markedly to the blue of the B band of ZnP and zinc tetrabenzoporphyrin.[13,15]

The calculated spectra for the H_3Ph_8Cz, $(OH^-)_2P^VPh_8Cz$ and $(OH^-)_2P^VMeO_8TBC$ model compounds exhibit a marked red shift of the main π → π* bands relative to those of H_3Cz, $(OH^-)_2P^VCz$ and P^VTBC

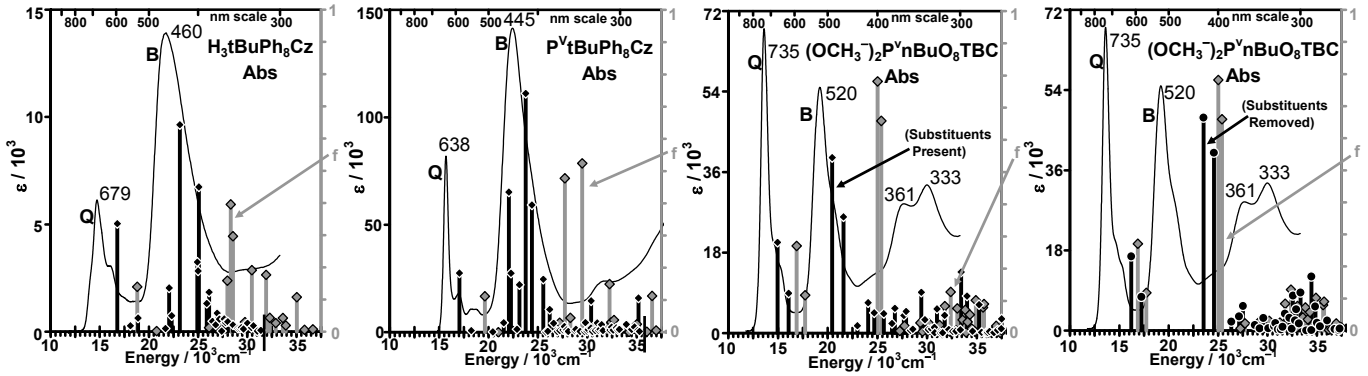

Figure 4. The UV-visible absorption spectra of **H_3tBuPh$_8$Cz**, **[(OH$^-$)P^{V}tBuPh$_8$Cz]$^+$OH$^-$** and **(OCH$_3^-$)$_2$P^{V}nBuO$_8$TBC**. An energy scale is used with a wavelength scale provided at the top of each plot and the wavelengths of the major bands are annotated. The first three plots from left to right contain calculated absorption spectra based on TD-DFT calculations for H_3Cz, (OH$^-$)$_2$P^{V}Cz and (OH$^-$)$_2$P^{V}TBC with no substituents (gray) and phenyl or MeO (black) groups are plotted against the right hand axes (Figure 1 and Table 2). The plot on the right contains the calculated spectra for the planar (OH$^-$)$_2$P^{V}TBC model complex (gray diamonds) and for the corresponding structure obtained once the substituents are removed from the optimized geometry of (OH$^-$)$_2$P^{V}MeO$_8$TBC to provide a non-planar (OH$^-$)$_2$P^{V}TBC structure (black circles) so the effect of the steric hindrance between the neighboring MeO groups across the direct pyrrole C–C bond can be assessed.

and greater complexity in the B band regions of H_3Ph$_8$Cz and (OH$^-$)$_2$P^{V}Ph$_8$Cz due to configuration interaction involving states associated with the phenyl rings (Figure 4). Since there is limited evidence for multiple pairs of coupled $\mathcal{B}_0$ terms in the B band region of **H_3tBuPh$_8$Cz**, **[(OH$^-$)P^{V}tBuPh$_8$Cz]$^+$OH$^-$**and **(OCH$_3^-$)$_2$P^{V}nBuO$_8$TBC**, it seems safe to conclude that the geometry optimizations of the H_3Ph$_8$Cz, [(OH$^-$)P^{V}Ph$_8$Cz]$^+$ model compound and ion (Figures 1 and 4 and Table 3) do not provide an accurate enough description of the structure as a basis for TD-DFT calculations given the conformational flexibility that exists in solution (Figure 2). Non-planarity induced by steric hindrance between neighboring –OR groups on either side of the direct C–C bond between neighboring pyrrole rings, Figure 2, is predicted to result in only a minor portion of the red shift of the Q and B bands of (OH$^-$)$_2$P^{V}MeO$_8$TBC relative to (OH$^-$)$_2$P^{V}Cz (Figure 4). This suggests that there is a significant substituent effect in the case of **(OCH$_3^-$)$_2$P^{V}nBuO$_8$TBC**. Despite the fact that the TD-DFT calculations are not in close agreement with the experimental data when the peripheral substituents are included in the case of **H_3tBuPh$_8$Cz** and **[(OH$^-$)P^{V}tBuPh$_8$Cz]$^+$OH$^-$**, the calculations for the model complexes clearly demonstrate that the one-electron transitions associated with the four frontier π–MOs within Michl's perimeter model,[10] Table 1, continue to play a major role in determining the optical properties of corrolazines. The assignment of the major bands to forbidden and allowed Q and B transitions using the band terminology originally adopted in Gouterman's 4-orbital model[9] for the D_{4h} symmetry metal porphyrins, is straightforward on this basis, Figures 1 and 4. A marked intensification of the Q bands is observed relative to the B bands in the MCD spectra of **H_3tBuPh$_8$Cz**, **[(OH$^-$)P^{V}tBuPh$_8$Cz]$^+$OH$^-$** and

$(OCH_3^-)_2P^VnBuO_8TBC$, Figure 1, as is the case with ZnPc, as would be anticipated based on the larger excited state magnetic moments predicted for the Q transitions based on Michl's perimeter model.[10]

An analysis of the spectroscopy of **H_3tBuPh_8Cz** and **$[(OH^-)P^VtBuPh_8Cz]^+OH^-$** provides the basis for studying the optical spectroscopy and electronic structure of transition metal MCz complexes. The spectra are comprised entirely of $n \rightarrow \pi^*$ and $\pi \rightarrow \pi^*$ bands with none of the ligand to metal and metal to ligand charge transfer (LMCT and MLCT) and $d \rightarrow d$ bands, which can be expected when there is a transition metal present with a partially filled d block (Table 3). Although the absorption spectrum of **$Mn^{III}tBuPh_8Cz$** is superficially similar to that of **$[(OH^-)P^VtBuPh_8Cz]^+OH^-$**, there are clearly marked differences in the MCD spectrum (Figure 1). A positive Faraday $\mathcal{B}_0$ term associated with a shoulder to the red of the main absorption band in the Q band region at 685 nm is almost certainly associated with a charge transfer band and the presence of an additional charge transfer band is the most likely explanation for the pair of negative $\mathcal{B}_0$ terms at 501 and 458 nm. The assignment of these bands is not straightforward given the large number of possible LMCT, MLCT and $d \rightarrow d$ transitions. A detailed analysis of a wide range of MCz and MTBC complexes, based on room and low temperature MCD spectral measurements will be required before definitive band assignments can be attempted.

In conclusion, despite the removal of an aza-nitrogen atom, key information about the electronic structure of MCz and MTBC complexes can still clearly be derived from MCD spectra. The semi-empirical approaches, which have been applied previously to MP and MPc complexes, such as Gouterman's 4-orbital model[9] and Michl's perimeter model,[10] are still applicable. The forbidden and allowed nature of the Q and B bands, based on the orbital angular momentum properties of the inner cyclic perimeter, is retained in the case of the $C_{15}H_{15}^{3-}$ parent hydrocarbon perimeter. The identification of Crl and Cz chromophores as soft MCD chromophores with $\Delta HOMO \approx \Delta LUMO$, Tables 1 and 2, means that complexes of these ligands are now prime candidates for perimeter model studies similar to those of Djerassi and coworkers on the effects of peripheral substituents on the optical spectroscopy and electronic structure of chlorins and bacteriochlorins.[16] It should be noted that in future a more quantitative approach to these studies will be much more feasible based on the development of TD-DFT based calculations for MCD intensity based on the three Faraday terms, which is currently under way.[17]

EXPERIMENTAL

The synthesis of **H_3tBuPh_8Cz**, **$[(OH^-)P^VtBuPh_8Cz]^+OH^-$**, **$Mn^{III}tBuPh_8Cz$** and **$(OCH_3^-)_2P^VnBuO_8TBC$** has been reported previously.[4] Electronic absorption spectra were measured with a Jasco V-570 spectrophotometer. Magnetic circular dichroism (MCD) spectra[11] were recorded using a Jasco J-725 spectrodichrometer and a Jasco electromagnet that produces a magnetic field of up to 1.09 T. Geometry optimizations, Figure 2, and TD-DFT calculations for the H_3Cz, H_3Ph_8Cz, $[(OH^-)P^VCz]^+$, $(OH^-)_2P^VCz$,

$(OCH_3^-)_2Ph_8P^VCz$, $(OH^-)_2P^VTBC$, model compounds and ion and for $C_{16}H_{16}^{2-}$, $C_{15}H_{15}^{3-}$, ZnP, ZnPc and ZnPz were carried out using the B3LYP functional of the G03W software package[18] with 6-31G(d) basis sets. A semi-empirical PM3 approach was used for 3,6,10,13,17,20,24,27-octamethoxy-triazaztetrabenzocorrolazine ($(OH^-)_2P^VMeO_8TBC$) prior to TD-DFT calculations for structures with and without MeO substituents.[18] The TD-DFT calculations for the $(OCH_3^-)_2Ph_8P^VCz$ model complex were based on coordinates from an X-ray structure.[4]

ACKNOWLEDGEMENTS

This research was partially supported through a Grant−in−Aid for Exploratory Research (No. 19655045 to N.K.), and a Grant−in−Aid for the COE project, Giant Molecules and Complex Systems, 2006 (to N.K.) from the Ministry of Education, Science, Sports and Culture, Japan. A portion of the computational results were obtained using supercomputing resources at the Information Synergy Center at Tohoku University. The authors thank this computational facility for their generous allotment of computer time. D.P.G. is grateful to the National Science Foundation, USA (CHE0606614) for partial support of this work.

REFERENCES AND NOTES

1. R. Paolesse, 'The Porphyrin Handbook,' Vol. 2, ed. by K. M. Kadish, K. M. Smith, and R. Guilard, Academic Press, Inc., London, 2000, pp. 201-231; D. P. Goldberg, *Acc. Chem. Res.*, 2007, **40**, 626; W. D. Kerber and D. P. Goldberg, *J. Inorg. Biochem.*, 2006, **100**, 838; D. P. Goldberg, J. P. Fox, D. T. Gryko, *J. Porphyrins Phthalocyanines*, 2004, **8**, 1091.
2. C. Erben, S. Will, and K. M. Kadish, in 'The Porphyrin Handbook,' Vol. 2, ed. by K. M. Kadish, K. M. Smith, and R. Guilard, Academic Press, Inc., London, 2000, pp. 232-300; R. Guilard, J.-M. Barbe, C. Stern, and K. M. Kadish, 'Handbook of Porphyrins and Related Macrocycles,' Vol. 18, ed. by K. M. Kadish, K. M. Smith, and R. Guilard, Academic Press, Inc., London, 2003, pp. 303-351.
3. S. Nardis, D. Monti, and R. Paolesse, *Mini Rev. Org. Chem.*, 2005, **2**, 355.
4. B. Ramdhanie, C. L. Stern, and D. P. Goldberg, *J. Am. Chem. Soc.*, 2001, **123**, 9447; B. S. Mandimutsira, B. Ramdhanie, R. C. Todd, H. Wang, A. A. Zareba, R. S. Czernuszewicz, and D. P. Goldberg, *J. Am. Chem. Soc.*, 2001, **123**, 9447; J. P. Fox, B. Ramdhanie, A. A. Zareba, R. S. Czernuszewicz, and D. P. Goldberg, *Inorg. Chem.*, 2004, **43**, 6600.
5. M. Fujiki, H. Tabei, and K. Isa, *J. Am. Chem. Soc.*, 1986, **108**, 1532.
6. J. Li, L. R. Subramanian, and M. Hanack, *Chem. Commun.*, 1997, 679; J. Li, L. R. Subramanian, and M. Hanack, *Eur. J. Org. Chem.*, 1998, 2759.
7. N. Kobayashi, F. Furuya, G.-C. Yug, H. Wakita, and M. Yokomizo, *Chem. Eur. J.*, 2002, **8**, 1474; N. Kobayashi, M. Yokoyama, A. Muranaka, and A. Ceulemans, *Tetrahedron Lett.*, 2004, **45**, 1755.

8. X^- is used throughout to denote an anionic axial ligand.
9. M. Gouterman, 'The Porphyrins,' Vol. III Part A, ed. by D. Dolphin, Academic Press, Inc., New York, 1978, pp. 1-165.
10. J. Michl, *J. Am. Chem. Soc.*, 1978, **100**, 6801; J. Michl, *Pure Appl. Chem.*, 1980, **52**, 1549.
11. J. Mack, M. J. Stillman, and N. K. Kobayashi, *Coord. Chem. Rev.*, 2007, **251**, 429.
12. W. J. Moffitt, *Chem. Phys.*, 1954, **22**, 320.
13. J. Mack, Y. Asano, N. Kobayashi, and M. J. Stillman, *J. Am. Chem. Soc.*, 2005, **127**, 17697.
14. R. M. Hochstrasser, *Acc. Chem. Res.*, 1968, **1**, 266.
15. J. Mack and M. J. Stillman, *J. Phys. Chem.*, 1995, **99**, 7935; J. Mack and M. J. Stillman, 'Handbook of Porphyrins and Related Macrocycles,' Vol. 16, ed. by K. M. Kadish, K. M. Smith, and R. Guilard, Academic Press, Inc., London, 2003, pp. 43−116.; V. N. Nemykin, R. G. Hadt, R. V. Belosludov, H. Mizuseki, and Y. Kawazoe *J. Phys. Chem. A* 2007, **111**, 12901.
16. J. D. Keegan, A. M. Stolzenberg, Y. C. Lu, R. E. Linder, G. Barth, A. Moscowitz, E. Bunnenberg, and C. Djerassi, *J. Am. Chem. Soc.*, 1982, **104**, 4305; J. D. Keegan, A. M. Stolzenberg, Y. C. Lu, R. E. Linder, G. Barth, A. Moscowitz, E. Bunnenberg, and C. Djerassi, *J. Am. Chem. Soc.*, 1982, **104**, 4317; C. Djerassi, Y. Lu, A. Waleh, A. Y. L. Shu, R. A. Goldbeck, L. A. Kehres, C. W. Crandell, A. G. H. Wee, A. Kniezinger, R. Gaete-Holmes, G. H. Loew, P. S. Clezy, and E. Bunnenberg, *J. Am. Chem. Soc.*, 1984, **106**, 4241; R. A. Goldbeck, *Acc. Chem. Res.*, 1988, **21**, 95.
17. M. Seth, T. Ziegler, A. Banerjee, J. Autschbach, S. J. A. van Gisbergen, and E. J. Baerends, *J. Chem. Phys.*, 2004, **120**, 10942; G. A. Peralta, M. Seth, and T. Ziegler, *Inorg. Chem.*, 2007, **46**, 9111; M. Seth, J. Autschbach, and T. Ziegler, *J. Chem. Theory Comput.*, 2007, **3**, 434.
18. Gaussian 03 (RevisionC.02), M. J. Frisch, G. W. Trucks, H. B. Schlegel, G. E. Scuseria, M. A. Robb, J. R. Cheeseman, J. A. Montgomery, Jr., T. Vreven, K. N. Kudin, J. C. Burant, J. M. Millam, S. S. Iyengar, J. Tomasi, V. Barone, B. Mennucci, M. Cossi, G. Scalmani, N. Rega, G. A. Petersson, H. Nakatsuji, M. Hada, M. Ehara, K. Toyota, R. Fukuda, J. Hasegawa, M. Ishida, T. Nakajima, Y. Honda, O. Kitao, H. Nakai, M. Klene, X. Li, J. E. Knox, H. P. Hratchian, J. B. Cross, V. Bakken, C. Adamo, J. Jaramillo, R. Gomperts, R. E. Stratmann, O. Yazyev, A. J. Austin, R. Cammi, C. Pomelli, J. W. Ochterski, P. Y. Ayala, K. Morokuma, G. A. Voth, P. Salvador, J. J. Dannenberg, V. G. Zakrzewski, S. Dapprich, A. D. Daniels, M. C. Strain, O. Farkas, D. K. Malick, A. D. Rabuck, K. Raghavachari, J. B. Foresman, J. V. Ortiz, Q. Cui, A. G. Baboul, S. Clifford, J. Cioslowski, B. B. Stefanov, G. Liu, A. Liashenko, P. Piskorz, I. Komaromi, R. L. Martin, D. J. Fox, T. Keith, M. A. Al-Laham, C. Y. Peng, A. Nanayakkara, M. Challacombe, P. M. W. Gill, B. Johnson, W. Chen, M. W. Wong, C. Gonzalez, and J. A. Pople, Gaussian, Inc., Wallingford CT, 2004.